Process Compensated Resonance Testing (PCRT) Inversion for Material Characterization and Digital Twin Calibration

Alexander Mayes[2,a)], Julieanne Heffernan[2,b)], Leanne Jauriqui[2,c)], Richard Livings[2,d)], Eric Biedermann[2,e)], John C. Aldrin[3,f)], Brent R. Goodlet[4,g)], Siamack Mazdiyasni[1,h)]

[1]Air Force Research Laboratory (AFRL/RXCA), Wright-Patterson AFB, OH, USA
[2]Vibrant Corporation, Albuquerque, NM, USA
[3] Computational Tools, Gurnee, IL, USA
[4]University of California, Santa Barbara, Santa Barbara, CA, USA

[a)] Corresponding author: amayes@vibrantndt.com
[b)] jheffernan@vibrantndt.com
[c)] ljauriqui@vibrantndt.com
[d)] rlivings@vibrantndt.com
[e)] ebiedermann@vibrantndt.com
[f)] aldrin@computationaltools.com
[g)] bgoodlet@engineering.ucsb.edu
[h)] siamack.mazdiyasni@us.af.mil

Abstract. The Digital Twin paradigm is based on the idea that a component's serviceable life and performance can be better predicted and monitored by creating a faithful virtual counterpart of a real component, which in turn leads to improvements in end-product safety and cost. Such a model requires accurate inputs for the initial material state of the part as well as in-service loads and damage states throughout its service life. The resonance frequencies of a part correlate to a part's material state and damage state. Similarly, changes in resonance frequencies correlate to changes in the part's material state resulting from in-service loads and damage. Process Compensated Resonance Testing (PCRT) leverages these physical relationships to perform nondestructive evaluation (NDE) and material characterization using the measured resonance frequencies of a component. Prior work has established techniques for modeling the effects of material property variation, crystal orientation, and damage states on resonance, as well as quantifying uncertainty propagation from model inputs to outputs. This study examines the use of PCRT model inversion to obtain material properties and calibrate digital twins of real components. Digital twin instances were first created for a population of single crystal Nickel-base superalloy samples using dimension and mass measurements. Then, after collecting resonance spectra from the physical counterparts, model inversion techniques were employed to estimate elastic properties and crystal orientation for each part. The digital twins were then calibrated with the model inversion output. These digital twins were subsequently validated by comparing the inversion results to resonance and x-ray diffraction measurements on a statistically significant population of physical specimens. The results highlight the value of part-specific material properties for digital twin performance, as well as the ability of PCRT to evaluate and improve digital twin fidelity.

INTRODUCTION

The purpose of this study was to evaluate the use of Process Compensated Resonance Testing (PCRT) model inversion to characterize a specific part or component and apply the obtained properties to a digital twin instance of that component. In brief, a digital twin is a complete virtual representation of a physical part or process [1]. For a given component a digital twin instance entails a simulation complete with details, not just for that part or assembly number but for that particular component's serial number, encompassing processes and operations it has undergone and expected future service Modeling a component to this level of detail can reduce the uncertainty present in probabilistic approaches, potentially resulting in improved safety and efficiency [2]. An ideal digital twin can provide information on expected operational performance, part lifing, maintenance recommendations, and likely defects or sources of damage. To do so, part specific information such as dimensions, operational history, maintenance history, and material state must be regularly fed back into the model.

Figure 1 presents a diagram of this information flow for an example turbine blade and its hypothetical digital twin instance. Some of the necessary data from such physical parts can be provided by in-situ with sensors [3,4], allowing real-time feedback and predictions from the model. Some properties, such as material state, are more difficult to measure and require offline inspections. Such testing can also serve to calibrate the digital twin, verifying that the model is representative of actual operational conditions and adjusting it to be closer to ground truth to improve the accuracy of future analyses. PCRT is one such inspection that has been shown to be sensitive to a part's material state over its service history [5] and can provide a quantitative metric to determine digital twin fidelity.

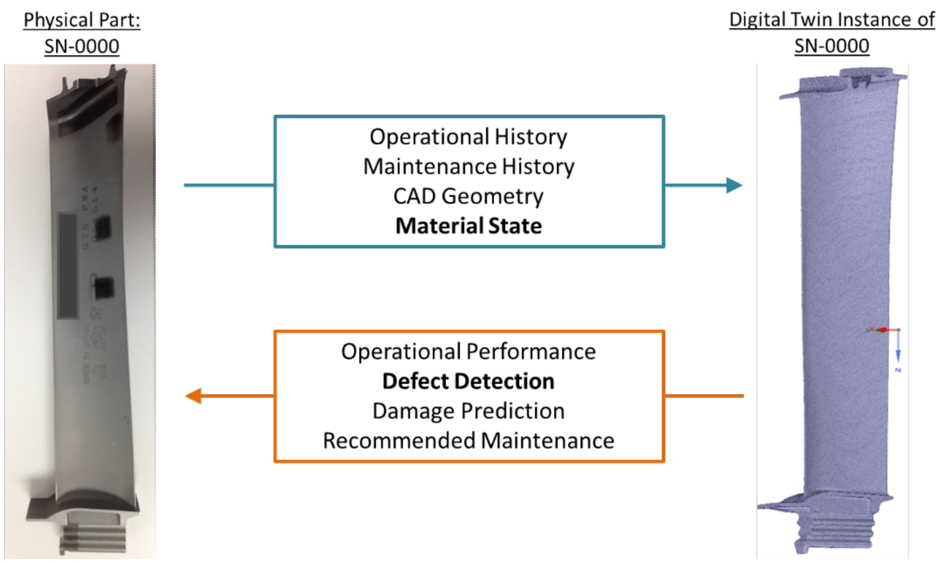

Figure 1. Diagram of data flow between the physical part and its digital twin instance.

PCRT is a non-destructive evaluation (NDE) method involving the collection and analysis of a part's resonance spectrum to evaluate its material or damage state [6]. Historically, applications of PCRT have evaluated parts on a pass or fail basis by comparing the part's resonance spectrum to a database of spectra recorded from a training population of characterized acceptable and unacceptable components. PCRT's pattern recognition algorithms are trained to recognize the pattern of diagnostic resonance modes that most effectively differentiate acceptable and unacceptable parts. Statistical scoring tools apply an objective, quantitative analysis of the resonance frequency data to render an automated pass or fail result that does not require interpretation [7]. While this approach has demonstrated its effectiveness in numerous operational NDE applications [8,9], it is often desirable to more fully characterize a defective part to better understand the nature and root cause of the defect/damage. To this end, recent PCRT research has focused on developing modeling capabilities to better predict the effects of changes in material, geometry, or even damage states on the resonance frequencies, and to improve PCRT capabilities for characterizing material states from resonance frequency measurements [10-13].

Using the finite element method (FEM), a part's resonance frequencies can readily be simulated for a given set of defining parameters. The inverse problem, determining a part's defining parameters from its resonance frequencies, is often not as straightforward. Model inversion using resonant ultrasound spectroscopy (RUS) is an established solution to this problem but has largely been limited to characterizing bulk elastic properties in simple coupon geometries [14-15]. Recent work in developing RUS has addressed samples of arbitrary geometry [16,17], multiple misaligned crystals [18,19], defects and damage states [11,20], and the use of FEM to enhance RUS capabilities [8,21]. By introducing FEM forward modeling, the inversion problem can be expanded to cover more complex geometries, materials, and damage states. Leveraging these expanded capabilities, PCRT model inversion can help to calibrate digital twin instances with otherwise hard to measure, part-specific material properties and evaluate model quality by comparing modeled-to-measured resonance frequencies. The following study details an experiment to demonstrate this approach by generating digital twin instances for 80 real samples, calibrating their material properties with inversion, evaluating the pre- and post-calibration models with resonance comparison, and verifying the crystal orientation findings with Laue X-ray diffraction.

METHODS

PCRT Model Inversion

Model inversion, in the context of PCRT, refers to determining the material state of a component by fitting a modeled prediction of resonance frequencies based on known material state information to the component's measured resonance spectrum. The material state parameters from the best fit model describe the material state of the physical part. The best fit model is obtained by iteratively modeling frequencies from different combinations of parameters until there is a satisfactory match between the simulated and measured frequencies. Figure 2 shows this process in more detail.

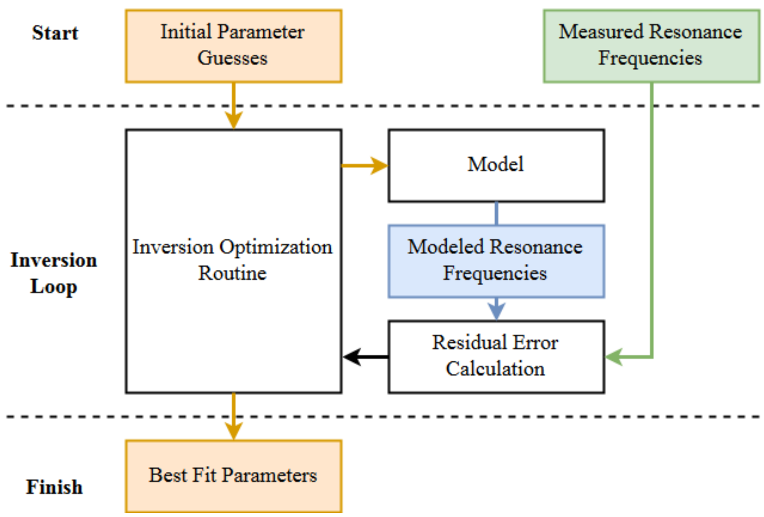

Figure 2. Diagram of PCRT model inversion

To begin, the measured resonance frequencies of the sample are passed to the inversion code, along with initial guesses for the parameter values. These initial parameters can be educated guesses based on literature or random guesses within constraints appropriate to the problem. The initial parameters are then passed to the inversion model, which calculates the resonance frequencies for that set of parameters. The modeled frequencies are then compared to the measured sample frequencies and the root-mean-square of the residual errors (RMSE) is passed to the optimization routine. The optimization routine makes changes to the parameter values based on the RMSE. The process is repeated until a convergence criterion has been met: either the RMSE is below a certain threshold or is not changing appreciably with further iterations. For this study, a non-linear least squares approach was taken for optimization using a trust-region-reflective algorithm [22]. Because non-linear least squares estimation is not guaranteed to find a global solution, multiple repetitions of each inversion were performed using different initial values. Initial values were chosen pseudo-randomly using Latin hypercube sampling to ensure that the full range of parameter values in the given bounds was represented [23]. The repetition with the lowest RMSE was designated as the best fit solution. Conventional wisdom in traditional RUS inversion of simple geometries holds that RMSE below 0.2% constitutes a good fit [24], though recent work for more complex geometries has found RMSE in the neighborhood of 0.5% to be more typical [25].

The model historically used in resonance inversion is an energy minimization technique that finds resonances of a solid body by approximating solutions of the mechanical Lagrangian [14-15]. While this approach is computationally inexpensive, it is limited to elastically homogenous material models and simple geometries such as spheres, rectangular parallelepipeds, and cylinders. To perform inversion of more complex geometries, material characteristics, and damage states, an FEM modeling approach was implemented. Because FEM has a relatively high computational cost per model evaluation, and the inversion model must be evaluated with every iteration, a meta-model was created to serve as the inversion model. This meta-model quickly interpolates over a pre-generated set of FEM model solutions [25]. While this approach introduces some additional uncertainty in the form of meta-model interpolation error, it provides fast inversion while still taking advantage of FEM's ability to model complex parts.

Digital Twin Generation and Evaluation

For the purposes of this study, a digital twin instance of a particular sample consists of a computer assisted design (CAD) 3D solid model and a FEM model, including mesh and material properties. The scope of this work covers the use of a digital twin to accurately simulate part resonances for later use in PCRT sort training and evaluating model fidelity for any further analyses. Because the frequency value for each resonance mode is the principal metric evaluated in PCRT, a list of resonance frequencies is the chief output of interest for these models, though mode shape information is also extracted for diagnostic purposes. To obtain resonance frequencies for a digital twin instance, first the 3D solid model of the nominal geometry is updated with sample-specific dimensions. This geometry is passed to ANSYS Workbench (ANSYS Inc., Canonsburg, PA) which creates a mesh. A modal analysis creates mass and stiffness matrices from the mesh, along with specified material properties and crystal orientation parameters, and extracts the requested mode information using a block Lanczos solver. The fidelity of the digital twin instance is then evaluated by comparing the frequencies of the modeled resonance modes to those measured with PCRT. Because resonance is directly related to a part's elastic properties, a strong agreement between modeled and measured frequencies indicates that the digital twin will behave realistically in subsequent analyses operating within the elastic regime.

EXPERIMENTAL SETUP

To assess the applicability of using PCRT model inversion to calibrate the digital twin, inversion was performed on a validation set of 80 physical specimens to estimate sample-specific material properties. Two sets of digital twin instances were then created: one using standard book-value elastic properties [26] and estimated crystal orientations, and the second using the best-fit inversion results for elastic properties and crystal orientation. The sets were evaluated by comparing their error from the measured resonance frequencies and follow-up analysis was performed on several samples highlighted with this process.

The samples used for this study were 80 ASTM E139-compliant axisymmetric dogbones of the geometry pictured in Figure 3. Dimensions of interest are called out and were chosen for their significant influence on resonance and ease of measurement. The coupons were designed and machined by Metcut Research Inc. for use in a parallel creep study [12]. All samples were machined in pairs from six-inch cast bars of single-crystal Mar-M-247, a nickel-base superalloy with cubic crystal symmetry. The three independent elastic parameters were defined as: elastic modulus in the <001> direction (E_{001}), Poisson's ratio in the <001> direction (ν_{001}), and Zener's anisotropy ratio (A) [27]. Due to the axisymmetric nature of the geometry, crystal orientation was fully defined with two independent variables using sequential Euler rotations. These rotations, shown in Figure 3, were defined (in order): θ, the angle between the crystal <001> and the long axis of the part, and ρ, the angle of rotation about the crystal <001>.

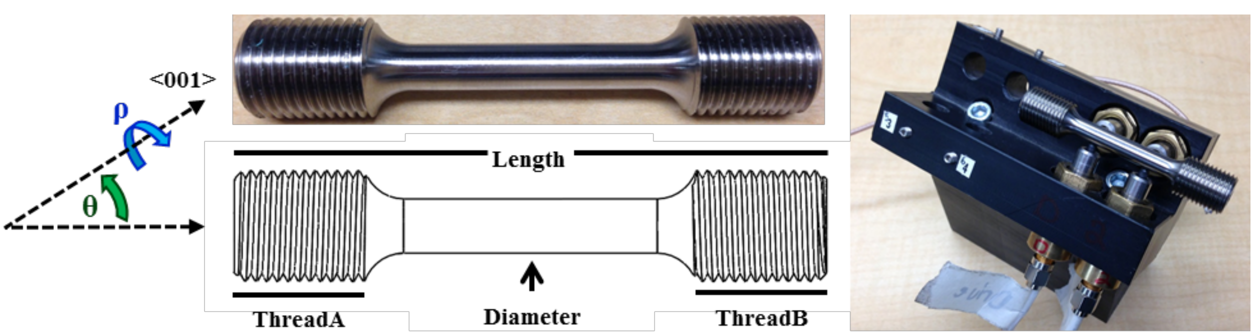

Figure 3. Dogbone sample geometry, dimensions of interest, crystal orientation angles, and PCRT fixturing

For all samples, mass measurements were taken with a scale and dimensions were measured with calipers or micrometers when possible. Though crystal orientations were not measured directly for each sample, Laue x-ray diffraction was performed by the casting vendor measuring the surface crystal orientation of the original cast bars. Each casting produced two dogbones and it was initially assumed that both resultant samples would have similar orientations to the parent casting. Resonance spectra were collected with a typical PCRT engineering fixture, shown in Figure 3. One piezoelectric transducer induced a swept sine wave across the frequency range of interest, 1.5 - 241 kHz in this case, and two additional transducers were used to measure the response. For this dogbone part, 34 measured resonance modes, corresponding to modeled modes 7-40, were identified as having satisfactory repeatability and quality for analysis.

The frequencies from these modes were used as input for PCRT model inversion. Additionally, mass and dimension measurements were included as constraints to reduce the number of unknown variables in the inversion. This is also somewhat necessary for good convergence; a set of parameters completely describing elastic properties, mass, or geometry can independently produce the same effect on frequency. If all of these parameters are left as unconstrained variables, the inversion problem can become ill-posed. By constraining mass and geometry, their effects on frequency were accounted for and this ill-posedness was avoided. Table 1 provides a range of nominal values for all the parameters included in the inversion meta-model. To create the meta-model, 162 FEM models were generated by sparsely sampling the ranges listed, and a 10-dimensional polynomial hyper-surface model was applied to the frequency data.

Table 1. Model input parameters and values for the dogbone inversion space

Parameter	Range	Min	Base	Max
E_{001} (GPa)	± 10.00%	115.00	127.73	140.56
ν_{001}	± 20.00%	0.30	0.37	0.45
A	± 20.00%	2.20	2.75	3.30
θ (°)	0-45.00	0.00	0.00	45.00
ρ (°)	± 45.00	-45.00	0.00	45.00
Mass (g)	± 0.33%	39.62	39.75	39.88
$L_{end\text{-}end}$ (mm)	± 0.33%	69.77	70.00	70.23
D_{gage} (mm)	± 0.84%	5.97	6.02	6.07
L_{thread} (A & B, mm)	± 3.29%	14.70	15.20	15.70

RESULTS AND DISCUSSION

Inversion Results

Table 2 summarizes the best fit inversion values for elastic properties and crystal orientation for all 80 measured samples and compares them to expected book values. Overall, elastic properties were aligned well with known properties of Mar-M-247 but, as expected, some part-to-part variations were observed. These variations reflect subtle differences present in the microstructure due to differences in the aggregate material behavior – differences that should be accounted for in a high-fidelity digital twin. Additionally, Table 2 provides an overview of the residual frequency error. The vast majority of inversions fit within 0.5% RMSE, giving confidence in the parameter estimates. These error metrics can also be informative for identifying outlier parts against the group.

Table 2. Summary of inversion results for the dogbone samples

Parameter	Best Fit Value		Book Values [26]
	Mean	Deviation	
Frequency RMSE	0.27%	0.19%	
E_{001} (GPa)	126.32	1.37%	127.54
ν_{001}	0.38	3.53%	0.39
A	2.78	3.67%	2.73
θ (°)	13.61	11.14	
ρ (°)	21.28	14.02	

Figure 4 plots the best fit θ and RMSE by part index, allowing closer examination of particular samples. Also, θ estimates provided by Laue of the parent castings are included in Fig. 4. Based on these results, the samples with the highest RMSE tended to also have the largest disagreement between cast Laue θ and best fit inversion θ. Additionally, several pairs of dogbones cut from the same casting were found to have very different θ values, calling into question the assumption of constant crystal orientation throughout the casting. Possible explanations for these disagreements include poor inversion fits or discrepancies between the Laue measurements and the true crystal orientations. Crystal deviations from the Laue measurements of a casting could be caused by Laue operator error, grain drift or twist, the presence of large secondary grains leading to one of the cut samples having a significant volume of material at a different orientation, or secondary grains on the casting surface that were later machined off.

To investigate these discrepancies further, four samples were selected for additional analysis (highlighted in Figure 4). The samples were chosen based on the following criteria as well as their unexpected behavior in a parallel study [12]:

- Sample 6 exhibited a large difference in resonance from its cast counterpart (Sample 5) and a noticeably poorer inversion fit by RMSE.
- Sample 13, along with its counterpart (Sample 14), consistently fit to θ = 13-14° despite having a cast Laue measurement of θ = 8.7°.
- Sample 53 exhibited a difference in resonance from its counterpart (Sample 54) and both had somewhat higher RMSE.
- Sample 66 was chosen as a reference for its low RMSE and good agreement between the cast Laue measurement and inversion.

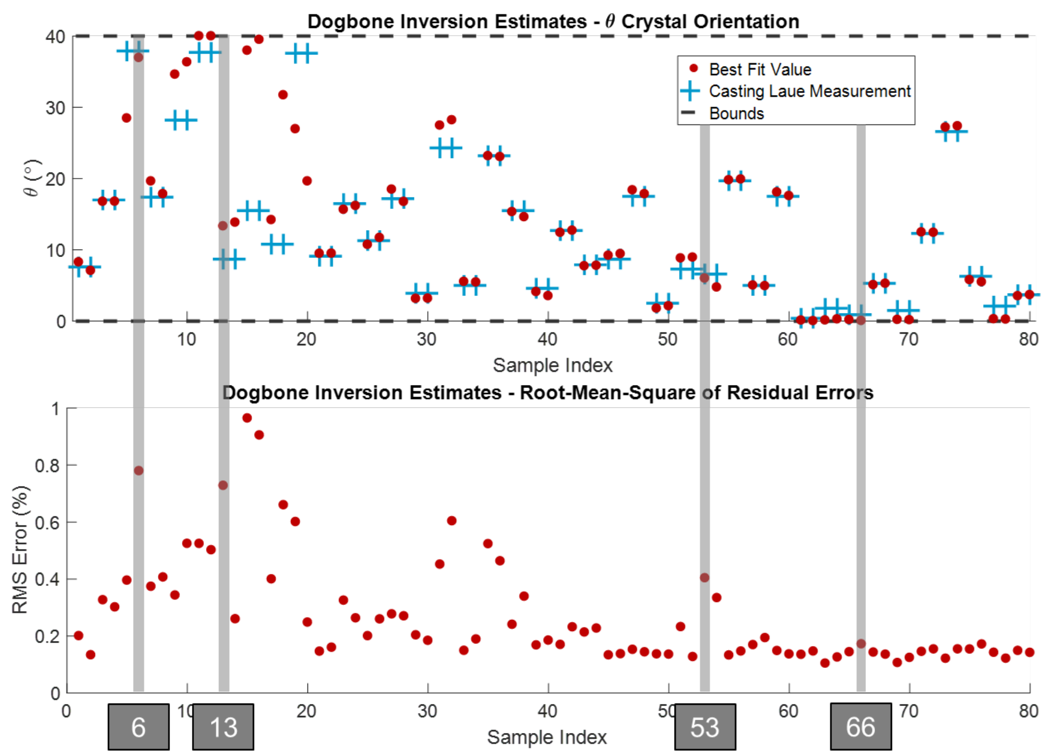

Figure 4. Best fit inversion results for crystal orientation angle θ and residual frequency error by sample. Four parts are highlighted for further analysis

Verification of Laue Diffraction

To better characterize the four samples chosen for further investigation, follow-up Laue measurements were performed in their final, machined state. Table 3 compares the casting vendor's measurement of the initial casting, the best fit inversion result, and the follow-up measurement for each machined part. Each sample was remeasured on both ends (labeled as Side A and Side B in the table) to evaluate possible orientation differences through the sample. Samples 6 and 53 both showed an almost 7° difference in θ between Side A and Side B when re-measured. This indicated significant grain drift or the presence of secondary grains, which corresponded to the difference between the inversion results and the original Laue measurements. Sample 13 showed a slight difference between sides, but both were considerably closer to the inversion estimate than the cast measurement. This difference, though less than 1°, may still be indicative of a crystal defect, which would also explain the higher RMSE seen in this sample. These results demonstrated that PCRT model inversion can accurately estimate orientation and that inversion fit quality can be used as an indicator of crystal anomalies within a part, including detection of parts that have been inaccurately classified by Laue measurements.

Table 3. Crystal orientation measurement, inversion, and re-measurement for select samples.

	θ Orientation Angle			
Part	**Cast Bar Laue**	**Inversion**	**Re-Laue Side A**	**Re-Laue Side B**
Sample 6	37.9°	37.0°	37.0°	30.4°
Sample 13	8.7°	13.3°	13.3°	14.1°
Sample 53	6.6°	6.0°	7.7°	14.1°
Sample 66	0.9°	0.0°	0.5°	0.6°

Digital Twin Instances

Figure 5 compares error metrics of the initial digital twin instances, modeled with book value material properties and Laue orientation estimates, to the inversion-improved digital twin instances, modeled with best fit material properties and orientations. The plot shows the average model-to-measure residual error by mode with error bars representing one standard deviation. In the initial models, many of the later modes showed good agreement between modeled and measured data, with averages centering around zero and deviations within 1%. However, a number of the earlier modes had very wide deviations, indicating that more than a few of the models matched relatively poorly. In the improved models, average residual error improved marginally for most of the modes, though there was still an offset in modes 7-12. The cause of this offset is unclear, though higher error in lower modes is common in PCRT model-to-measure comparisons and may be attributed to error associated with part fixturing. The standard deviation of errors improved across the entire range, with the most significant improvement in the modes that had exhibited wider error bars in the initial models. This likely reflects the significant improvement in modeling parts that may have been misclassified by Laue crystal orientations measurements in their as-cast state, or whose material properties were further away from nominal book values. Overall, the improved models had an average model-to-measure frequency error of -0.19% ± 0.41% across all modes.

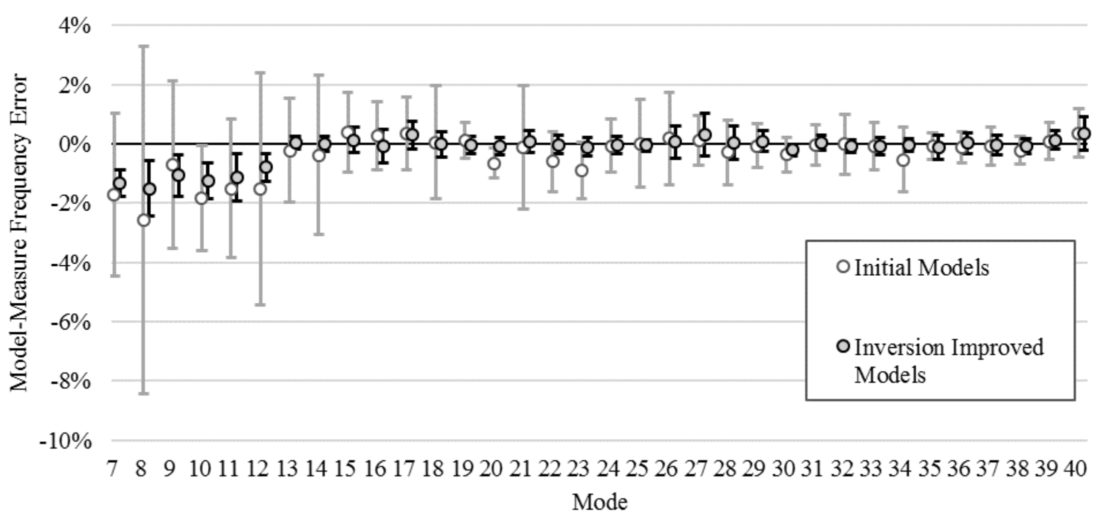

Figure 5. Average and standard deviation of residual error by mode for initial and inversion improved digital twin instances

Figure 6 plots the model-to-measure errors for two of the samples-of-interest highlighted in the previous section. Sample 13 showed improvement in almost all modes, transforming from a model with a poor match to real data to one with a fairly good match. Given the difference in orientation between the models ($\theta_{initial} = 8.7°$ vs. $\theta_{improved} = 13.3°$), this likely indicates that the Laue estimation of orientation based off the casting for this part was incorrect and inversion adjusted the digital twin to be closer to ground truth. Sample 6 also showed across the board improvement, though high error remained in a handful of modes. Remaining high residual errors, such as that seen in mode 11 for Sample 13 and modes 27 and 29 for Sample 6, likely indicate something that inversion was unable to account for, possibly anomalies like grain drift or secondary grains that were not included in the model.

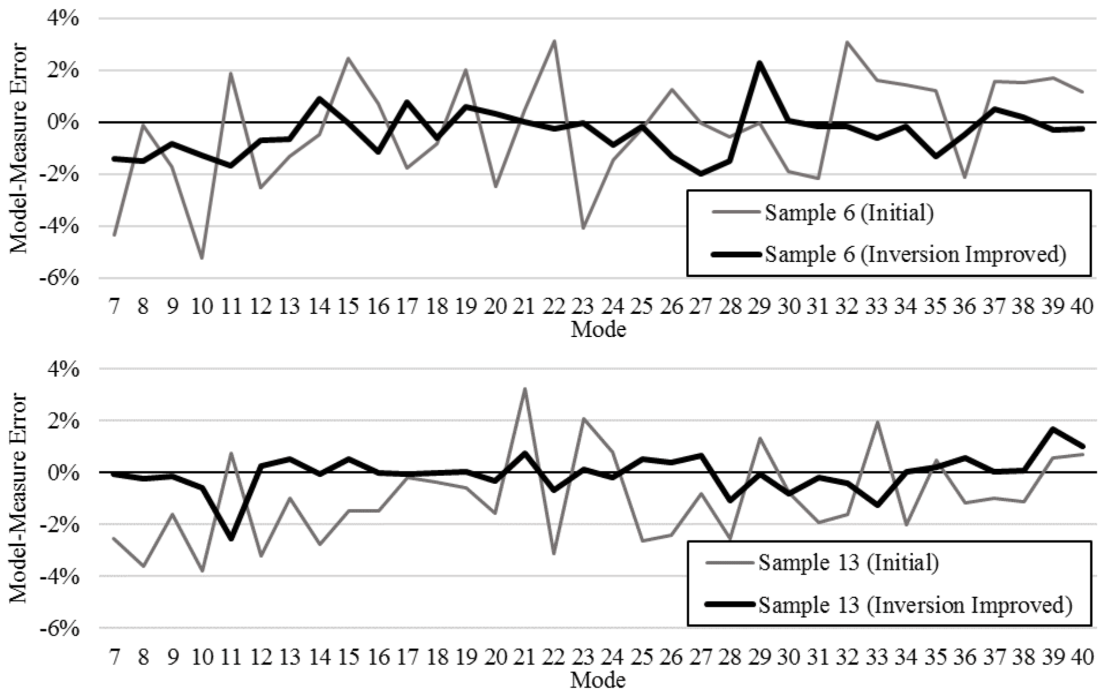

(a)

(b)

Figure 6. Model-to-measure frequency error by mode index for (a) sample 6 and (b) sample 13.

CONCLUSION

This study evaluated PCRT model inversion as a means of calibrating a digital twin with part-specific material properties and proposed using resonance frequency model-to-measure error as a metric for evaluating digital twin fidelity. Inversion of the measured resonance frequencies resulted in mostly acceptable fits with good alignment to established material properties for the nickel-base superalloy Mar-M-247. Digital twin instances were created for the samples, first using book value material properties and crystal orientations estimated from Laue measurements of castings, and then calibrated with best fit values from the model inversion. Calibration was shown to have a significant improvement in model-to-measure error of resonance frequencies. Verification Laue performed on select parts of interest found that inverted crystal orientations were closer to ground truth than the initial Laue estimations, reflected by a tighter match between modeled and measured resonances, and that large remaining residual errors were indicative of crystal anomalies not accounted for in the FEM model. These results illustrate the value of using PCRT model inversion to calibrate digital twin instances and the effectiveness of resonance frequency residual error as a means of measuring model fidelity and highlighting potential problems. PCRT is easy to deploy at the production and depot levels (many facilities already use it for routine inspection), and its ability to quantify otherwise difficult-to-measure properties and verify model accuracy makes it a valuable tool in supporting the digital twin ecosystem.

ACKNOWLEDGEMENTS

This research was supported by the U.S. Air Force Research Laboratory (AFRL) through a Materials and Manufacturing Directorate (AFRL/RX) Structural Materials Broad Agency Announcement (BAA) Contract FA8650-15-C-5208 and an AFRL Small Business Innovation Research (SBIR) Phase II Contract, FA8650-15-C-5074. This paper has been cleared for public release under case number: 88ABW-2018-4872.

REFERENCES

1. E. H. Glaessgen and D. S. Stargel, “The digital twin paradigm for future NASA and U.S. Air Force vehicles,” *53rd Structures, Structural Dynamics, and Materials Conference*, pp. 1–14, Honolulu, Hawaii, (2012).
2. Li, Chenzhao & Mahadevan, Sankaran & Ling, You & Wang, Liping & Choze, Sergio, “A Dynamic Bayesian Network Approach for Digital Twin,” *19th AIAA Non-Deterministic Approaches Conference*, AIAA Sci-Tech Forum, AIAA 2017-1566, (2017).
3. M. Dowell, G. Sylvester, R. Krupp, and G. Zipfel, “Progress in Turbomachinery Prognostics and Health Management via Eddy Current Sensing,” *2000 IEEE Aerospace Conference Proceedings*, IEEE, (2000)
4. I. Garcia, J. Zubia, G. Durana, G. Aldabaldetreku, and M. A. Villatoro, “Optical Fiber Sensors for Aircraft Structural Health Monitoring,” *Sensors*, **15**, pp. 15494-15519, (2015).
5. D. Piotrowski, L. Hunter, and T. Sloan, “Process Compensated Resonance Testing JT8D-219 1st Stage Blades,” *ATA NDT Forum 2008*, (2008), avaliable at: http://www.vibrantndt.com/wp-content/uploads/Delta-TechOps-Vibrant-casestudy.pdf.
6. ASTM Standard E2534-15, (2015), “Standard Practice for Process Compensated Resonance Testing via Swept Sine Input for Metallic and Non-Metallic Parts, ASTM International, www.astm.org.
7. J. Schwarz, J. Saxton, and L. Jauriqui, “Process Compensated Resonant Testing in Manufacturing Process Control,” *Material Evaluation*, **63**, pp. 736-739, (2005).
8. D. M. Craig, “NDT Technology Readiness: A P&WC Case Study,” *2016 Airlines for America NDT Forum*, (2016), available at: http://airlines.org/wp-content/uploads/2016/11/9_28_1100.pdf
9. D. Piotrowski, G. Weaver, “Enhancing Reliability with Process Compensated Resonance Testing (PCRT) at Delta TechOps,” *2016 Airlines for America NDT Forum*, (2016), available at: http://airlines.org/wp-content/uploads/2016/10/9_28_1315.pdf.
10. E. Biedermann, J. Heffernan, A. Mayes, G. Gatewood, L. Jauriqui, B. Goodlet, T. Pollock, C. Torbet, J. C. Aldrin, and S. Mazdiyasni, “Process Compensated Resonance Testing Modeling for Damage Evolution and Uncertainty Quantification,” *43rd Annual Review of Progress in QNDE,* AIP Conf. Proc, **1806**, pp. 090005, (2017).
11. J. Heffernan, L. Jauriqui, E. Biedermann, A. Mayes, R. Livings, B. Goodlet, and S. Mazdiyasni, “Process compensated resonance testing models for quantification of creep damage in single crystal nickel-based superalloys” *Materials Evaluation*, **75**, n 7, pp. 941-952, (2017).
12. J. Heffernan, E. Biedermann, A. Mayes, R. Livings, L. Jauriqui, and S. Mazdiyasni, “Validation of Process Compensated Resonance Testing (PCRT) Sorting Modules with Modeled Data,” *45th Annual Review of Progress in QNDE*, AIP Conf. Proc, (expected 2019).
13. R. Livings, A. Mayes, E. Biedermann, J. Heffernan, L. Jauriqui, B. Goodlet, and S. Mazdiyasni, “Detection of Microtexture Regions in Titanium Turbine Engine Disks using Process Compensated Resonance Testing: A Modeling Study,” *45th Annual Review of Progress in QNDE*, AIP Conf. Proc. (expected 2019).
14. A. Migliori, J. Sarrao, M. W. Visscher, T. Bell, M Lei, Z. Fisk, and R. Leisure, ‘‘Resonant ultrasound spectroscopy techniques for measurement of the elastic moduli of solids,’’ *Physica B*, **183**, pp. 1–24, (1993).
15. A. Migliori, and J. L. Sarrao, *Resonant Ultrasound Spectroscopy*, New York, Wiley, (1997).
16. G. Liu, and J. D. Maynard, “Measuring elastic constants of arbitrarily shaped samples using resonant ultrasound spectroscopy,” *Journal of the Acoustical Society of America*, **131**, n. 3, pp. 2068-2078, (2012).
17. M. C. Remmillieux, T. J. Ulrich, C. Payan, J. Riviere, C. R. Lake, and P.-Y. Le Bas, “Resonant ultrasound spectroscopy for materials with high damping and samples with arbitrary geometry,” *Journal of Geophysical Research: Solid Earth*, **120**, pp. 4898-4916, (2015).
18. L. H. Rettberg, B. R. Goodlet, T. M. Pollock, “Detecting recrystallization in a single crystal Ni-base alloy using resonant ultrasound spectroscopy,” *NDT & E International*, **83**, pp. 68-77, (2016).

19. T. J. Lesthaeghe, R. A. Adebisi, S. Sathish, M. R. Cherry, and P. A. Shade, “Toward characterization of single crystal elastic properties in polycrystalline materials using resonant ultrasound spectroscopy,” *Materials Evaluation*, **75**, n 7, pp. 930-940, (2017).
20. B. R. Goodlet, C. J. Torbet, E. Biedermann, L. Jauriqui, J. C. Aldrin, and T. M. Pollock, “Forward models for extending the mechanical damage evaluation capability of resonant ultrasound spectroscopy,” *Ultrasonics*, **77**, pp. 183-196, (2017).
21. J. Plesek, R. Kolman, and M. Landa, “Using finite element method for the determination of elastic moduli by resonant ultrasound spectroscopy,” *Journal of the Acoustical Society of America*, **116**, n. 1, pp. 282-287, (2004).
22. Web site: https://www.mathworks.com/help/optim/ug/choosing-the-algorithm.html#bsbwx1l
23. R. L. Iman, J. M. Davenport, D. K. Zeigler, *Latin Hypercube Sampling (Program User’s Guide)*, Albuquerque, Sandia Laboratories and Texas Tech University, (1980).
24. A. Migliori and J. D. Maynard, “Implementation of a Modern Resonant Ultrasound Spectroscopy System for the Measurement of the Elastic Moduli of Small Solid Specimens,” *Review of Scientific Instruments*, AIP, **76**, pp. 121301, (2005).
25. J. C. Aldrin, A. Mayes, L. Jauriqui, E. Biedermann, J. Heffernan, R. Livings, B. Goodlet, S. Mazdiyasni, “Uncertainty Quantification of Resonant Ultrasound Spectroscopy for Material Property and Single Crystal Orientation Estimation on a Complex Part,” *44th Annual Review of Progress in QNDE*, AIP Conf. Proc., **1949**, pp. 140010, (2018).
26. Kuhn, H-A. and Sockel, H-G, “Elastic Properties of Textured and Directionally Solidified Nickel-based Superalloys Between 25 and 1200° C,” Materials Science and Engineering, A112, 177-126, (1989).
27. C. Zener, *Elasticity and Anelasticity of Metals*, Chicago, University of Chicago, (1948).